International Journal For Advanced Research In Science & Technology
A peer reviewed international journal
www.ijarst.in
ISSN: 2457-0362

NEOTERICS PREPARATION OF PLGA LOADED NEDAPLATIN NANOPARTICLES BY VARIOUS DATA ANALYSIS

Senkuttuvan Ilanchit Chenni[1], Dr. Kathiresan Suresh[2], Dr. Palanivel Venkatesan[3], Dr. Nagappan Kannappan[4], Dr. Muthusamy Rajasekar[5], Abulkalam Asath Nihal Ahamed[6], Ravichandran Pugazhendhi[7]

[1,6,7]Department of Biochemistry and Biotechnology, Annamalai University, Annamalai Nagar, Chidambaram, Tamil Nadu 608002, India.
[2] Associate Professor, Department of Biochemistry and Biotechnology Annamalai University, Annamalainagar – 608 002, Tamilnadu, India
[3,4]Department of Pharmacy, Annamalai university, Annamalai University, Annamalai Nagar, Chidambaram, Tamil Nadu, 608002, India
[5]Central Research Laboratory for Biomedical Research, Vinayaka Missions' Kirupananda Variyar Medical College and Hospitals, Salem 636308 India.

suraj_cks@yahoo.co.in , ilanchitchenni30@gmail.com venkatesan1978@gmail.com , kannappanpharmacy@gmail.com , nihalahamed2013@gmail.com , pugazhmyr@gmail.com

Abstract

Poly-(D, L-lactic-co-glycolic) acid (PLGA)-loaded nedaplatin nanoparticles (PLGA-NDP) were prepared. The details of the preparation and characterisation of PLGA-loaded Nedaplatin nanoparticles formed and optimised by the double emulsion technique and Box–Behnken design with poly-(D, L-lactic-co-glycolic) acid as a polymer and polyvinyl alcohol (PVA) as surfactant agents were investigated. The morphology and elemental distribution, physical state, internal structure, encapsulation efficiency, and release profile were examined through sequential tactics such as Scanning Electron Microscopy-Energy Dispersive X-ray, Dynamic light scattering, Thermogravimetric analysis- Differential thermal analysis, Fourier-Transform Infrared Spectroscopy, UV-VIS spectroscopy, and in-vitro drug release study, respectively. Four factors at four levels were used in the Box-Behnken design to calculate the central point. The interaction between these factors significantly enhanced the results. The response of the optimised condition provided an accurate prediction, and the experiment was conducted further. The design was validated, and satisfactory agreement was observed between the predicted and experimental values. The obtained results provide evidence of a new geometric construction of PLGA-loaded nedaplatin nanoparticles with enhanced efficiency when compared to the reported research articles related to nedaplatin in cancer studies. Therefore, these findings and techniques are useful for the preparation of NPs.

Keywords: • Drug Delivery Systems, • Double Emulsion Technique; • Poly-(D, L-lactic-co-glycolic) acid; • Nedaplatin; • Box-Behnken design

1. INTRODUCTION

Investigations in modern drug research have highlighted the importance of biodegradable polymer nanoparticles as drug delivery systems to enhance bioavailability while maintaining therapeutic efficacy **[1]**. Nanoparticles are integral in nanotechnology,

especially for drug delivery. In cancer treatment, nanoparticles serve as anticancer agent carriers, using passive and active targeting at the tumour site **[2,3]**. Passive targeting relies on the accumulation of therapeutic agents, despite differences between carcinomas and normal tissues. Rezvantalab et al. (2018), Danaei et al. (2018), and Yetisgin et al. (2020) reported that vascular and lymphatic dysfunction results in increased permeability and retention effect (EPR), aiding transportation and retention of therapeutic nanoparticles. Nanoparticle uptake into the targeted or mucosal barrier is limited **[3–5]**. Nanoparticle properties, including size, shape, and surface charge, affect the EPR effect, influencing circulation duration, penetration rate, and cellular internalisation. Physiochemical properties also affect nanoparticle extravasation and accumulation **[6]**. Polymer nanoparticles are optimal for sophisticated drug delivery systems, aiming to improve therapeutic and rehabilitative efficacy. Polymeric nanoparticles with surfactants enhance drug delivery stability, controlled release, particle size, site targeting, bioavailability, biocompatibility, physical properties, and preservation of pharmaceutical molecules from threats and environmental degradation **[7]**.

An effective method is the response surface methodology (RSM), which includes central composite design (CCD), Box–Behnken design (BBD), and D-optimal design. BBD was used to optimise the formulation of nanoparticles to minimise particle size and maximise yield, encapsulation efficiency, and drug release. The BDD design provides a superior illustration of intervariable reactions and optimises these factors with reduced time and minimal experimental effort **[8–10]**. Nedaplatin (cis-diamine-glycoplatinum) is a derivative of cisplatin, first reported in Japan in 1983. Its antineoplastic potency treats various tumours, including head and neck, oesophageal, uterine, ovarian, and lung cancers **[11]**. In clinical studies in Japan, Nedaplatin has shown remarkable therapeutic efficacy against head and neck, lung, and cervical cancers, with lower renal and gastrointestinal toxicity compared to Cisplatin **[12,13]**.

Poly- (D, L-lactic-co-glycolic) acid (PLGA) polymer was selected for its superior drug carrier properties, including encapsulation efficiency, reduced adverse effects, and prevention of drug degradation. Cancer development and progression can be influenced by factors such as disruption of tumour suppressor genes, irregular cellular differentiation, and malfunctioning apoptosis caused by excessive proliferation**[14,15]**. While nanoformulation has advanced significantly, various research areas require attention, including precise manipulation of nanostructures, scalable synthesis techniques, enhancement of functionalisation methods, environmental sustainability, and data-centric synthesis strategies. In this study, the properties of PLGA encapsulating nedaplatin were examined to reach the therapeutic efficacy.

MATERIALS AND METHODS

Poly-(D, L-lactic-co-glycolic) acid (PLGA) [Nomisma Healthen Pvt. ltd], cis-di ammine(glycolate) platinum II (Nedaplatin) [Sigma Aldrich], polyvinyl alcohol (PVA) [MP Biomedical], dichloromethane [MP Biomedical], phosphate-buffered saline (PBS) [Lonza], and dialysis membranes [HI media] were purchased.

International Journal For Advanced Research In Science & Technology
A peer reviewed international journal
www.ijarst.in
ISSN: 2457-0362

2.1 Nanoparticles Preparation

Nedaplatin-loaded nanoparticles were prepared using a water-oil-water emulsion solvent evaporation method, with minor modifications. For the primary solution, nedaplatin (6mg) was emulsified in dichloromethane composed of PLGA (18mg). The primary emulsion was added to the aqueous phase containing PVA (2% w/v) and continuously homogenized (95 Å, 20 min). The evaporation of dichloromethane occurred during continuous homogenization. The nanoparticles (PLGA-NDP) were collected by centrifugation, washed with sterile water, freeze-dried using an optimized protocol, and stored at -20°C until further use [16].

Software The experimental design, statistical analysis and desirability function calculation were developed using STST-EASE DESIGN EXPERT VERSION 13.

2.2 Nanoparticle Morphology

The nanoparticle morphology and constituent elements were examined using scanning electron microscopy (SEM)- EDX (JEOL, JSM- IT200). The samples were spotted on double-sided tape and sputter-coated with a five nm-thick gold layer [15].

2.3 Size, Polydispersity Index and Zeta Potential

The potential average particle size, zeta potential, and polydispersity index of the nanoparticles were determined by Dynamic Light Scattering using a Malvern instrument. The analysis was performed in the potential range of -120 to 120V at 25°C and a scattering angle of 90°; the samples were appropriately diluted with ultra-purified water [17,18].

2.4 Thermal Assimilation

The physical state of the PLGA-loaded NDP nanoparticles was examined by thermal analysis (TG/DTA), carried out (SDT Q600 V20.9 Build 20, TA Instruments) in a nitrogen atmosphere at a heating rate of 20°C min-1 from 25 to 1000°C, using powder samples [19].

2.5 Determination of Drug content, Encapsulation Efficiency and Yield Percentage

The content of PLGA-encapsulated Nedaplatin was estimated using UV-Visible Spectroscopy. PLGA-NDP was dissolved in an aqueous solution, which was measured by UV Spectroscopy (SHIMADZU – UV 1800) at wavelength ranging from 200 to 800 nm. The percentage yield (% yield) and encapsulation efficiency (EE) were calculated using the following equations. [16,20,21]

$$Percentage\ yield\ (\%) = \frac{Weight\ of\ nanoparticles\ obtained}{total\ weight\ of\ drug\ and\ polymer\ added} \times 100 \qquad \text{(Equation 1)}$$

$$Encapsulation Efficiency(EE) = \frac{The\ total\ amount\ of\ drug\ added - Amount\ of\ dug\ in\ the\ supernatant}{total\ amount\ of\ drug\ added} \times 100 \text{ (Equation 2)}$$

2.6 Fourier-Transform Infrared Spectroscopy

Cisplatin, PLGA-loaded NDP nanoparticles, and nedaplatin were triturated separately with IR-grade KBr and compressed into thin pellets. The pellets were scanned over a range of 400–4000 cm^{-1}, and Fourier transform infrared (FTIR) spectra were recorded using an FTIR spectrometer (Perkin Elmer Model – Spectrum) [16].

2.7 In-Vitro Release of Nanoparticle compound

The dispensation of the nanoparticle was carried out in PBS medium according to a previously published method with minor modifications [22,23]. First, 6mg/ml of nanoparticles was resuspended in a dialysis membrane bag with a molecular cut-off of 12000-14000kDa. The membrane bag was placed in 50ml PBS (pH 7.4) under magnetic stirring at 120 rpm, and the temperature was maintained at 37°C. The amount of framed compound released from the dialysis bag was calculated at different time intervals (2, 4, 6, 8, 24 and 48hr) by measuring the absorbance at 226nm.

3. RESULTS

3.1.1 Outcome of Box-Behnken design arrangement for the formulation of PLGA-NDP nanoparticles:

Preparation optimized the drug to polymer ratio using the Box-Behnken design (BBD). Table 1 lists optimal values and responses for each factor. BBD minimized particle size, increased yield, encapsulation efficiency, and drug release, offering better intervariable reactions and optimized factors efficiently.

Seventeen formulation runs were performed with factors like polymer concentration, sonication time, and amplitude affecting yield, particle size, entrapment efficiency, and drug release. Tables 2 and 3 list optimal values and responses for each factor. This method calculated percentage yield, particle size, EE, and drug release, proving its significance. Drug-polymer concentration and sonication time were more influential than amplitude in determining nanoparticle yield. The interaction plot evaluated nanoparticle yield based on drug-polymer concentration and sonication time. The response fit a quadratic model validated by lack of fit, R2 test, and ANOVA, indicating good data fit. Colored dots on ramps depict the acceptable range of predicted variables. The overlay plot explored the effective variable region. A perturbation plot showed how changes in a single factor influenced the response, with other factors constant.

3.1.2 Result of Perturbation, Interaction, Predicted 3D response surface plot of Percentage of Yield of PLGA-NDP

Fig.1A shows yield is significantly influenced by drug-polymer concentration, impacted by sonication time and amplitude (b&c). This factor can achieve optimal yield. Significant deviations in the perturbation plot pinpoint key factors for the response. Fig.1B shows the interaction plot demonstrating a positive association between drug and polymer concentrations and sonication time. Nanoparticle yield was influenced by the correlation between polymer ratio and sonication time, suggesting yield was not solely determined by Drug-Polymer concentration. Fig.1C depicts the expected three-dimensional response surface

methodology plot for percentage yield. The 3D image shows a rise in yield percentage with extended sonication time. Drug-polymer concentration played a crucial role in yield increase, suggesting higher yield results from moderate sonication time and concentration.

3.1.3 Result of Perturbation, Interaction, Predicted 3D response surface plot of Particle Size of PLGA-NDP

The results showed particle sizes of 100-200nm were beneficial for drug permeation over oral mucosal tissue. The polydispersity index (PDI) describes size variation, with a higher PDI indicating wider distribution. Zeta potential can influence particle stability and mucoadhesion. Fig.2(A) indicates that drug-polymer concentration impacts sonication time and amplitude, reducing particle size. A greater deviance from the centre point identifies the relevant factor for the response. (B) Shows the interaction plot illustrating the relationship between drug and polymer concentrations and sonication time, determining particle size. (C) Depicts the expected three-dimensional response surface methodology plot for particle size. The 3D image showed particle size increased with extended sonication time and increased drug-polymer concentration.

3.1.4 Consequence of Perturbation, Interaction & Predicted 3D response surface plot of PLGA-NDP Encapsulation Efficiency

Fig.3A graph indicates drug-polymer concentration (a) influences sonication time (b) and amplitude (c), suggesting its importance for Encapsulation Efficiency. Greater deviance from the center point identifies relevant factors. Fig.3B shows encapsulation efficiency increased with increased sonication period and drug-polymer concentration, illustrating their positive relationship. This indicates both factors determined encapsulation efficiency. Fig. 3C's 3D image shows encapsulation efficiency increased with extended sonication time. Drug-polymer concentration significantly impacted Encapsulation Efficiency increase, revealing the increase was due to mid-level sonication time and concentration.

3.1.5. Result of Perturbation, Interaction & Predicted 3D response surface plot of Drug Release

Fig. 4.A shows the drug-polymer concentration factor attaining the best yield. Greater deviance from the centre point identifies the relevant factor for the response. An interaction plot determines factors producing percentage yield. Yield increased with sonication period and drug-polymer concentration. Fig. 4.B shows the interaction plot illustrating the positive relationship between drug-polymer concentrations and sonication time, indicating % yield was determined by both factors. Drug-polymer concentration significantly impacted Drug Release. Fig. 4.C depicts the 3D response surface methodology plot for Drug Release, showing increased Drug Release with extended sonication time and mid-level drug-polymer concentration.

Table 4 presents result of DLS: the particle size was 138 nm, PDI was 0.341, and zeta potential was -14.5 mV.

International Journal For Advanced Research In Science & Technology
A peer reviewed international journal
www.ijarst.in
ISSN: 2457-0362

3.2 Determination of Encapsulation Efficiency, and Percentage Yield

The obtained nanoparticle product was investigated using UV-visible spectroscopy at wavelengths of 200-800 nm wavelengths. The encapsulation efficiency (EE) and percentage yield (% yield) were obtained through BBD optimized factors. The table 5 shows the result of EE is 87.05% and % yield is 21.76%. Their values are similar to those reported in the literature [20,21].

3.3 Outcome of PLGA-NDP Nanoparticle Morphology

The nanoparticle morphology was studied using scanning electron microscopy (SEM). SEM-EDX, with energy-dispersive X-ray spectrometry (EDS), determines the chemical composition of materials. Fig. 5A shows spherical nanoparticles with a smooth surface. Fig. 5B reveals elements discerned by EDX at 2keV high-intensity peaks of platinum, confirming platinum nanoparticle formation. Other peaks correspond to elements present with the nanoparticles.

3.4 Outcome of thermal analysis of PLGA-NDP

Fig. 6 presents the TGA and DTA curves of the [PLGA-NDP] composite. The TGA curve shows PLGA-NDP decomposition under N2 purging to form PtNPs. Two significant mass changes were observed: one around 250°C, with a 2.5% loss, and another from 265°C to 350°C, with a 93.54% loss. From 400°C to 800°C, the weight remained constant at 3.126%, indicating all other materials degraded. The remaining weight corresponded to the platinum content. The DTA curve showed an endothermic peak at 317.03°C, attributed to the reduction process, forming platinum nanoparticles.

3.5 Fourier-Transform Infrared Spectroscopy of PLGA-NDP

Fig. 7 (a) shows the FTIR spectra of nedaplatin, prominent peaks were at 3423.90cm-1, 3293.35cm-1, 2923.34cm-1, 1622.40cm-1, 1369.97cm-1, and 1059.63cm-1. Peaks at 3423.90cm-1 and 3228.33cm-1 indicated (OH) hydrogen bond stretching. The peak from 2923.34cm-1 to 2855.69cm-1 was due to alkane stretching. The peak 2431.34cm-1 to 2026.85cm-1 indicated C≡C medial alkyne di-substituted stretching. The peak at 1622.40cm-1 was attributed to open-chain imino (-C=N-). Peaks at 1161.43cm-1 and 1115.76cm-1 indicated (C-N) amine, 927.20cm-1 and 903.12cm-1 (=C-H), 863.03cm-1 -NH2 and N-H wagging C shift on H bonding, 754.89cm-1 -O-H bend, and 673.37cm-1 to 519.22cm-1 aliphatic iodo compound C-I stretching.

Fig. 7 (b) shows the FTIR spectrum of cisplatin, distinguished peaks were at 3408.02cm-1, 1631.39cm-1, 1314.03cm-1, 1301.05cm-1, and 801.11cm-1. The peak at 3408.02cm-1 indicated hydrogen bonds or OH polymers causing OH/NH stretching. The peak from 2921.36cm-1 to 2104.7cm-1 was caused by CH methylene, S-H thids, and cyanide ion stretching. Peaks of 1534.39cm-1, 1418.24cm-1 to 1301.05cm-1 represented aromatic nitro compound, vinyl, OH phenol or tertiary alcohol, and C-H vinylidene stretching. Peaks of 1118.00cm-1, 1030.57cm-1, 872.99cm-1, 801.11cm-1, 668.08cm-1, 621.15cm-1, and

517.77cm-1 were associated with C-F aliphatic fluoro compound, (C-H) vinylidene, C-H 1,4 di-substitution C-Br aliphatic bromo compound, and (C-I) aliphatic iodo compound stretching. The peak at 473.93 cm-1 indicated poly sulfide (S-S) stretch.

Fig. 7 (c) the FTIR spectrum of PLGA-NDP, prominent peaks were at 3433.63cm-1, 2999.38cm-1, 2955.31cm-1, 2921.91cm-1, 1745.59cm-1, and 1631.87cm-1. Peaks at 3433.63cm-1 indicated hydrogen bonds or OH polymeric bonds, and the peak at 2999.38cm-1 to 2955.31cm-1 is attributed to (C-H) stretching mode. The peak at 2921.91cm-1, 2851.21cm-1, 2613.96cm-1, and 2025.90cm-1 were associated with methylene, CH3, methyne, and C-H overlap stretching. Peaks from 1745.59cm-1 to 1631.99cm-1, 1539.05cm-1, and 1513.99cm-1 were for aromatic combination and aromatic nitro compound stretch. Peaks at 1453.29cm-1, 1425.07cm-1, 1384.84cm-1, 1272.28cm-1, 1168.68cm-1, and 1095.78cm-1 indicated the presence of (C-H), (O-H), phenol or tertiary alcohol, (C-O), (C-O), and aliphatic fluoro compounds (C-F). The peak 957.78 cm-1 represented =C-H & =CH2, 889.90cm-1 and 870.29cm-1 of vinylidene C-H out of plane bend, 847.91cm-1 C-H 1,4-disubstitution, 749.21cm-1 and 720.90cm-1 of O-H bend out-of-plane. All FTIR results were depicted in Fig. 6A, B&C. The fingerprint regions of Nedaplatin, Cisplatin, and Poly-(D, L-lactic-co-glycolic) acid-loaded nedaplatin compounds were distinct; each was distinguished, and the peaks were in the form of an endothermic peak..

3.6 Outcome of In Vitro Kinetic Drug Release of PLGA-NDP

In nanoparticle studies drug release is the key factor, in which the slow release is attributed to the fact that solubilized or dispersed drugs can be released only slowly from the polymer matrix compared to the free drug. In present study Fig.8, the obtained drug release percentage (% of 66.07) was recorded at a slow rate with sustained release within 24hrs at 7.4 pH.

4. DISCUSSION

In drug delivery systems development, ensuring encapsulation efficiency is crucial for sufficient drug distribution to tissue targets. These characteristics can be managed by examining specific formulation and process factors [24]. This study used BBD to improve drug encapsulation efficiency, as in previous nanoparticle studies [10]. Preliminary research, literature, and equipment restrictions determined formulation factors. Optimum desirability was attained at mid-level drug-polymer concentration, sonication time, and maximum sonication amplitude [8,25].Particle size affects permeation across cell membranes and formulation stability. Large size distribution may cause aggregation, reducing drug release and permeation. Zeta potential indicates colloidal dispersion stability and inter-particle repulsion. Pronounced zeta potential values, positive (≥ 30mV) or negative (≤ -30mV), stabilize particle suspensions [17,19,26,27]. Present findings showed particle size of 138 nm, PDI of 0.341, and zeta potential of -14.5mV. Encapsulation efficiency was 87.05% and percentage yield was 21.76%, similar to literature values [28,29].

SEM is a powerful tool for analyzing sample morphology, aligning with previous studies. It provides high-magnification imaging for contamination identification, particle analysis, surface features, and texture [30]. Fig. 5A shows spherical nanoparticles with polished surfaces. Fig. 5B illustrates element identification through EDX, with high-intensity platinum peaks at 2keV, confirming platinum nanoparticle production using double emulsion.

The TGA curve showed weight percentage decreasing with temperature, indicating continuous mass change due to thermal treatment. The first decomposition started at a lower temperature and continued to a higher temperature with weight percentage change. The uniform curves in the last portion corresponded to material crystallization, with crystallization temperature varying for different compositions. Weight loss (%) decreased with increasing temperature due to different reactions [20,21]. FTIR spectroscopy is powerful for studying polymeric materials' structure and interactions with fillers. FTIR results for Nedaplatin, Cisplatin, and PLGA-NDP compounds were illustrated in Fig. 7A, B &C. Each compound's fingerprint regions were distinct, with peaks confirming the nanoparticle formulation's success.

"Unlike oral dosage forms that mimic body pH, nanoscale dosage forms' delivery vehicle depends on administration and action sites, making in vivo condition simulation tricky". Nanoparticle erosion during storage may increase drug release. Initial release increase may be due to drug attachment to the nanoparticle surface. Later stage slow release is attributed to drugs releasing slowly from the polymer matrix compared to free drug [16,21,31]. In this study, the profile was similar; 66.07% was recorded at a slow rate with sustained release within 24hrs at 7.4 ph. Thus PLGA-NDP appears to be a more effective cancer cell eliminator than Nedaplatin, making it promising for treating oral cancer.

5. CONCLUSIONS

In summary, Polymeric nanoparticle synthesis has advanced due to its potential for biodegradable and biocompatible structures for therapeutic delivery. Gaps remain in nanostructure control, scalable synthesis, functionalization, environmental sustainability, and data-driven approaches. This study addressed these gaps by developing methods to control size, shape, and morphology of polymeric nanoparticles (PNPs), creating scalable synthesis methods, improving PNP functionalization, and utilizing data science software to optimize synthesis. We employed the Double Emulsion technique to create a novel nanosphere preparation method that encapsulated nedaplatin in poly-(D, L-lactic-co-glycolic) acid. The size, encapsulation efficiency, and release profile of the encapsulated drug were confirmed. The PLGA-NDP nanoparticles can serve as novel therapeutic drug delivery agents in in-vitro and in-vivo studies.

ACKNOWLEDGMENT

The authors sincerely thank the Indian Council of Medical Research (ICMR) for providing financial assistance and the Department of Biochemistry and Biotechnology, Annamalai University, Annamalai Nagar- 608002, Tamil Nadu, India, for providing academic support to carry out this research successfully.

DECLARATION

Conflict of interest: The authors declare that there are no conflicts of interest.

DATA AVAILABILITY STATEMENT

Data supporting the findings of this study are accessible from the corresponding author upon reasonable request.

Abbreviations;

- PLGA - Poly- (D, L-lactic-*co*-glycolic) acid
- NDP- Nedaplatin
- PLGA-NDP – Poly- (D, L-lactic-*co*-glycolic) acid loaded Nedaplatin
- TGA-DTA – Thermogravimetric analysis- Differential thermal analysis
- EE – Encapsulation Efficiency
- SEM-EDX - Scanning Electron Microscopy- Energy Dispersive X-ray
- DLS- Dynamic light scattering
- DEM- Double Emulsion Method
- BBD- Box-Behnken design
- EFR- Enhanced Permeability and Retention Effect

REFERENCES

[1] M. Portaccio, C. Menale, N. Diano, C. Serri, D.G. Mita, M. Lepore, Monitoring production process of cisplatin-loaded PLGA nanoparticles by FT-IR microspectroscopy and univariate data analysis, J. Appl. Polym. Sci. 132 (2015) app.41305. https://doi.org/10.1002/app.41305.

[2] R. Dinarvand, N. Sepehri, Manouchehri, Rouhani, F. Atyabi, Polylactide-co-glycolide nanoparticles for controlled delivery of anticancer agents, Int. J. Nanomedicine (2011) 877. https://doi.org/10.2147/IJN.S18905.

[3] S. Rezvantalab, N.I. Drude, M.K. Moraveji, N. Güvener, E.K. Koons, Y. Shi, T. Lammers, F. Kiessling, PLGA-Based Nanoparticles in Cancer Treatment, Front. Pharmacol. 9 (2018) 1260. https://doi.org/10.3389/fphar.2018.01260.

[4] M. Danaei, M. Dehghankhold, S. Ataei, F. Hasanzadeh Davarani, R. Javanmard, A. Dokhani, S. Khorasani, M. Mozafari, Impact of Particle Size and Polydispersity Index on the Clinical Applications of Lipidic Nanocarrier Systems, Pharmaceutics 10 (2018) 57. https://doi.org/10.3390/pharmaceutics10020057.

[5] A.A. Yetisgin, S. Cetinel, M. Zuvin, A. Kosar, O. Kutlu, Therapeutic Nanoparticles and Their Targeted Delivery Applications, Molecules 25 (2020) 2193. https://doi.org/10.3390/molecules25092193.

[6] J.K. Patel, A.P. Patel, Passive Targeting of Nanoparticles to Cancer, in: Y.V. Pathak (Ed.), Surf. Modif. Nanoparticles Target. Drug Deliv., Springer International Publishing, Cham, 2019: pp. 125–143. https://doi.org/10.1007/978-3-030-06115-9_6.

[7] S. Chandran, V. Ravichandran, S. Chandran, J. Chemmanda, B. Chandarshekar, Biosynthesis of PVA encapsulated silver nanoparticles, J. Appl. Res. Technol. 14 (2016) 319–324. https://doi.org/10.1016/j.jart.2016.07.001.

[8] M.M. Ba-Abbad, P.V. Chai, A. Benamour, D. Ewis, A.W. Mohammad, E. Mahmoudi, Optimizing and control of effective synthesize parameters for Fe3O4 nanoparticles using response surface methodology, Chem. Pap. 76 (2022) 6359–6370. https://doi.org/10.1007/s11696-022-02320-y.

[9] N.M. Soliman, F. Shakeel, N. Haq, F.K. Alanazi, S. Alshehri, M. Bayomi, A.S.M. Alenazi, I.A. Alsarra, Development and Optimization of Ciprofloxacin HCl-Loaded Chitosan Nanoparticles Using Box–Behnken Experimental Design, Molecules 27 (2022) 4468. https://doi.org/10.3390/molecules27144468.

[10] S. Thrivikraman Nair, K. Kamalasanan, A. Moidu, P. Shyamsundar, L.J. Nair, V. P, Ethyl cellulose coated sustained release aspirin spherules for treating COVID-19: DOE led rapid optimization using arbitrary interface; applicable for emergency situations, Int. J. Biol. Macromol. 182 (2021) 1769–1784. https://doi.org/10.1016/j.ijbiomac.2021.05.156.

[11] P.P. Corbi, F. Cagnin, A.C. Massabni, Synthesis and characterization of a platinum(II) complex with N-acetyl- L -cysteine, J. Coord. Chem. 62 (2009) 2764–2771. https://doi.org/10.1080/00958970902942974.

[12] L. Yin, J. Wu, J. Wu, J. Ye, X. Jiang, M. Chen, D. Wang, X. Wang, D. Zong, J. Gu, J. Zhang, J. Wu, L. Xu, X. He, W. Guo, Radiosensitization Effect of Nedaplatin on Nasopharyngeal Carcinoma Cells in Different Status of Epstein-Barr Virus Infection, BioMed Res. Int. 2014 (2014) 1–7. https://doi.org/10.1155/2014/713674.

[13] S. Lu, Z. Chen, C. Hu, J. Zhang, Y. Chen, Y. Song, Q. Zhao, Y. Fan, G. Wu, Z. Ma, J. Fang, Q. Yu, Z. Liu, Nedaplatin Plus Docetaxel Versus Cisplatin Plus Docetaxel as First-Line Chemotherapy for Advanced Squamous Cell Carcinoma of the Lung — A Multicenter, Open-label, Randomized, Phase III Trial, J. Thorac. Oncol. 13 (2018) 1743–1749. https://doi.org/10.1016/j.jtho.2018.07.006.

[14] R.L. McCall, R.W. Sirianni, PLGA Nanoparticles Formed by Single- or Double-emulsion with Vitamin E-TPGS, J. Vis. Exp. (2013) 51015. https://doi.org/10.3791/51015.

[15] X. Xie, Q. Tao, Y. Zou, F. Zhang, M. Guo, Y. Wang, H. Wang, Q. Zhou, S. Yu, PLGA Nanoparticles Improve the Oral Bioavailability of Curcumin in Rats: Characterizations and Mechanisms, J. Agric. Food Chem. 59 (2011) 9280–9289. https://doi.org/10.1021/jf202135j.

[16] N. Alam, V. Khare, R. Dubey, A. Saneja, M. Kushwaha, G. Singh, N. Sharma, B. Chandan, P.N. Gupta, Biodegradable polymeric system for cisplatin delivery: Development, in vitro characterization and investigation of toxicity profile, Mater. Sci. Eng. C 38 (2014) 85–93. https://doi.org/10.1016/j.msec.2014.01.043.

[17] D.M. Calderón, U. Morales, C. Velásquez, V.H. Lara, L. Salgado, Thermal Decomposition of Diammonium Tetrachloroplatinate to form Platinum Nanoparticles and its Application as Electrodes, Catal. Lett. 132 (2009) 268–274. https://doi.org/10.1007/s10562-009-0106-9.

[18] T. Kahn, J. Bosch, M. Levitt, M. Goldstein, Effect of sodium nitrate loading on electrolyte transport by the renal tubule, Am. J. Physiol.-Leg. Content 229 (1975) 746–753. https://doi.org/10.1152/ajplegacy.1975.229.3.746.

[19] B.A. Miura, N.H. Ferreira, P.F. Oliveira, E.H. De Faria, D.C. Tavares, L.A. Rocha, K.J. Ciuffi, E.J. Nassar, Functionalization of luminescent YVO4:Eu3+ nanoparticles by sol–gel, J. Lumin. 159 (2015) 93–99. https://doi.org/10.1016/j.jlumin.2014.10.061.
[20] G. Chen, J. Wen, Poly(lactic-co-glycolic acid) based double emulsion nanoparticle as a carrier system to deliver glutathione sublingually, J. Biomed. 3 (2018) 50–59. https://doi.org/10.7150/jbm.27148.
[21] R. Khaira, J. Sharma, V. Saini, Development and Characterization of Nanoparticles for the Delivery of Gemcitabine Hydrochloride, Sci. World J. 2014 (2014) 1–6. https://doi.org/10.1155/2014/560962.
[22] A.R. Chandrasekaran, C.Y. Jia, C.S. Theng, T. Muniandy, S. Muralidharan, S. Arumugam, Invitro studies and evaluation of metformin marketed tablets-Malaysia, J. Appl. Pharm. Sci. (n.d.).
[23] A.R. Dudhani, S.L. Kosaraju, Bioadhesive chitosan nanoparticles: Preparation and characterization, Carbohydr. Polym. 81 (2010) 243–251. https://doi.org/10.1016/j.carbpol.2010.02.026.
[24] L.R. Tefas, I. Tomuţă, M. Achim, L. Vlase, Development and optimization of quercetin-loaded PLGA nanoparticles by experimental design, Clujul Med. 1957 88 (2015) 214–223. https://doi.org/10.15386/cjmed-418.
[25] A. Ganna, S.J. Vaithiyanathan, P. V P, V. P, Multiresponse Optimization of HPLC Method: Simultaneous Estimation of Protease Inhibitors and NNRTI in Human Plasma, J. Chromatogr. Sci. (2021) bmab067. https://doi.org/10.1093/chromsci/bmab067.
[26] A. Sarfraz, A.H. Raza, M. Mirzaeian, Q. Abbas, R. Raza, Electrode Materials for Fuel Cells, in: Encycl. Smart Mater., Elsevier, 2022: pp. 341–356. https://doi.org/10.1016/B978-0-12-803581-8.11742-4.
[27] A. Singh, K. Miyabayashi, Novel continuous flow synthesis of Pt NPs with narrow size distribution for Pt@carbon catalysts, RSC Adv. 10 (2020) 362–366. https://doi.org/10.1039/C9RA08762A.
[28] I. Muthuvel, K. Gowthami, G. Thirunarayanan, B. Krishnakumar, M. Swaminathan, R. Siranjeevi, Solar light-driven CeVO4/ZnO nanoheterojunction for the mineralization of Reactive Orange 4, Environ. Sci. Pollut. Res. 27 (2020) 43262–43273. https://doi.org/10.1007/s11356-020-10271-8.
[29] A.B.D. Nandiyanto, R. Oktiani, R. Ragadhita, How to Read and Interpret FTIR Spectroscope of Organic Material, Indones. J. Sci. Technol. 4 (2019) 97. https://doi.org/10.17509/ijost.v4i1.15806.
[30] S. Kashyap, A. Singh, A. Mishra, V. Singh, Enhanced sustained release of furosemide in long circulating chitosan-conjugated PLGA nanoparticles, Res. Pharm. Sci. 14 (2019) 93. https://doi.org/10.4103/1735-5362.253356.
[31] S. D'Souza, A Review of *In Vitro* Drug Release Test Methods for Nano-Sized Dosage Forms, Adv. Pharm. 2014 (2014) 1–12. https://doi.org/10.1155/2014/304757.

LEGENDS

Fig. 1 (A) Perturbation graph shows yield is significantly influenced by drug-polymer concentration (a) more than sonication time (b) and amplitude (c), suggesting drug-polymer

concentration achieves the best yield. The greater deviance from the center point identifies the relevant factor for the response. (B) Interaction plot shows a positive relationship between drug-polymer concentrations and sonication time, significantly affecting nanoparticle yield. (C) Expected 3D response surface methodology plot for percentage yield. The 3D image shows yield percentage increased with extended sonication time. Drug-polymer concentration significantly impacted yield increase, due to mid-level sonication time and drug-polymer concentration.

Fig. 2 (A) The graph indicates that drug-polymer concentration (a) influences sonication time (b) and amplitude (c), suggesting it can reduce particle size. This perturbation plot identifies the relevant factor for the response. (B) An interaction plot determines factors that interact to determine particle size, showing the positive relationship between drug and polymer concentrations and sonication time. This indicates particle size was determined by both drug polymer concentration and sonication period. (C) Depicts the expected three-dimensional response surface methodology plot for particle size. The 3D image indicated that when sonication time extended and drug-polymer concentration increased, particle size increased.

Fig. 3 (A) The graph shows that drug-polymer concentration (a) affects sonication time (b) and amplitude (c). (B) Encapsulation Efficiency of nanoparticles increased with longer sonication and higher drug–polymer concentration. (C) The 3D image indicates that extended sonication time significantly increased Encapsulation Efficiency, impacted by drug-polymer concentration.

Fig. 4 (A) The graph shows drug-polymer concentration (a) influences sonication time (b) and amplitude (c), suggesting the best yield. This perturbation plot identifies the relevant factor concerning the response. (B) The interaction plot illustrates the relationship between drug-polymer concentrations and sonication time, indicating % yield was determined by both. (C) The 3D response surface methodology plot shows Drug Release increased with extended sonication time. Drug-polymer concentration significantly impacted Drug Release at mid-level sonication time and concentration.

Fig. 5 (A) shows spherical nanoparticles with polished surfaces. Fig. 5B illustrates element identification through EDX, with high-intensity platinum peaks at 2keV, confirming platinum nanoparticle production using double emulsion.

Fig 6 (a) TGA curve showing thermal decomposition profile. Three distinct regions: (i) initial weight loss (~250°C, 2.5% loss), (ii) major weight loss (265-350°C, 93.54% loss, attributed to PLGA degradation), and (iii) constant weight (400-800°C, 3.126% residual weight, attributed to platinum nanoparticles. (b) DTA curve showing endothermic peak at 317.03°C, corresponding to reduction of platinum precursor and formation of platinum nanoparticles.

Fig. 7 A, B & C FTIR results for Nedaplatin, Cisplatin, and PLGA-NDP compounds show distinct fingerprint regions, with peaks confirming the nanoparticle formulation's success.

International Journal For Advanced Research In Science & Technology
A peer reviewed international journal
www.ijarst.in
ISSN: 2457-0362

Fig 8 graph depicts the in vitro release profile of PLGA-NPD from a dialysis membrane in PBS at pH 7.4 over 24 hours. The data shows a sustained-release pattern, with 66.07% of the drug released within 24 hours**.**

Figure and tables

Tables

Table 1 Box-Behnken design arrangement and four factors' responses for the formulation of PLGA-NDP nanoparticles

		Factor 1	Factor 2	Factor 3	Response 1	Response 2	Response 3	Response 4
Std	Run	A:Polymer con	B:Sonication Time	C:Sonication amplitude	% Yield	Particle Size	EE	Drug Release
			min			nm	%	%
1	13	2	10	85	73.2	149.2	80.3	87.6
2	9	10	10	85	83.1	291	88.6	90.7
3	2	2	30	85	81.2	247	87.6	88.4
4	17	10	30	85	87.9	204	93.6	92.3
5	11	2	20	75	77.6	394	75.6	89
6	14	10	20	75	89.3	281	87.3	82.3
7	3	2	20	95	81.4	161.7	87.7	75.6
8	7	10	20	95	86.3	311.2	85.7	70.8
9	4	6	10	78	75.2	336.7	80.1	87.5
10	12	6	30	75	79.9	209.3	79.3	78.5
11	8	6	10	95	81.5	152	82.4	77.4
12	6	6	30	95	89.3	241	76.9	78.6
13	15	6	20	85	89.3	138	82.4	82
14	16	6	20	85	89.3	138	82.4	82
15	5	6	20	85	86.8	138	82.4	82
16	10	6	20	85	89.3	138	82.4	82
17	1	6	20	85	89.3	138	82.4	82

Table 2 Parameter of factors analysis in BBD

Factor	Name	Units	Type	SubType	Minimum	Maximum	Coded Low	Coded High	Mean	Std. Dev.
A	Polymer con		Numeric	Continuous	2.00	10.00	-1 ↔ 2.00	+1 ↔ 10.00	6.00	2.83
B	Sonication	min	Numeric	Continuous	10.00	30.00	-1 ↔	+1 ↔	20.00	7.07

International Journal For Advanced Research In Science & Technology
A peer reviewed international journal
www.ijarst.in
ISSN: 2457-0362

	Time						10.00	30.00		
C	Sonication amplitude		Numeric	Continuous	75.00	95.00	-1 ↔ 75.00	+1 ↔ 95.00	85.18	6.84

Table 3 Response model and statistical parameter obtained from ANOVA of BBD

Response	Name	Units	Observations	Minimum	Maximum	Mean	Std. Dev.	Ratio
R1	% Yield		17.00	73.2	89.3	84.11	5.42	1.22
R2	Particle Size	nm	17.00	138	394	215.77	82.49	2.86
R3	EE	%	17.00	75.6	93.6	83.36	4.57	1.24
R4	Drug Release	%	17.00	70.8	92.3	82.86	5.77	1.30

Table 4. Summary of Particle Size, Polydispersity Index, and Zeta Potential

Name Of Nanoparticle	Particle Size	Polydispersity Index	Zeta Potential
PLGA- NDP	138 nm	0.341	- 14.5mV

Table 5 Summary of Encapsulation Efficiency (EE) and Percentage Yield (% yield)

Name Of Nanoparticle	Encapsulation Efficiency	Percentage yield
PLGA- NDP	87.05 %	21.76 %

Figure

Fig. 1. Perturbation, Interaction and Predicted 3D response surface plot of Percentage of Yield

International Journal For Advanced Research In Science & Technology
A peer reviewed international journal
www.ijarst.in
ISSN: 2457-0362

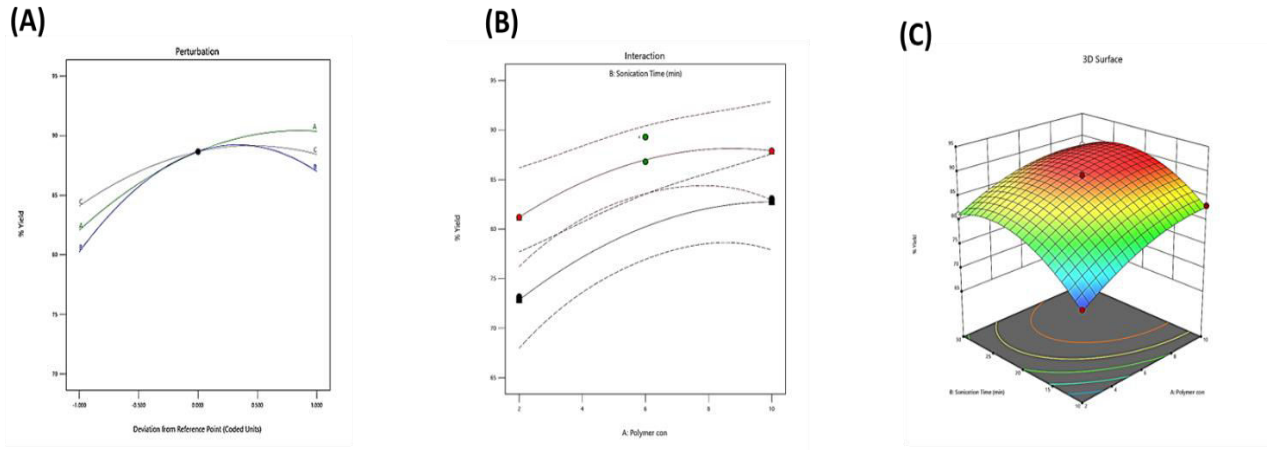

Fig. 2. Perturbation, Interaction, Predicted 3D response surface plot of Particle Size

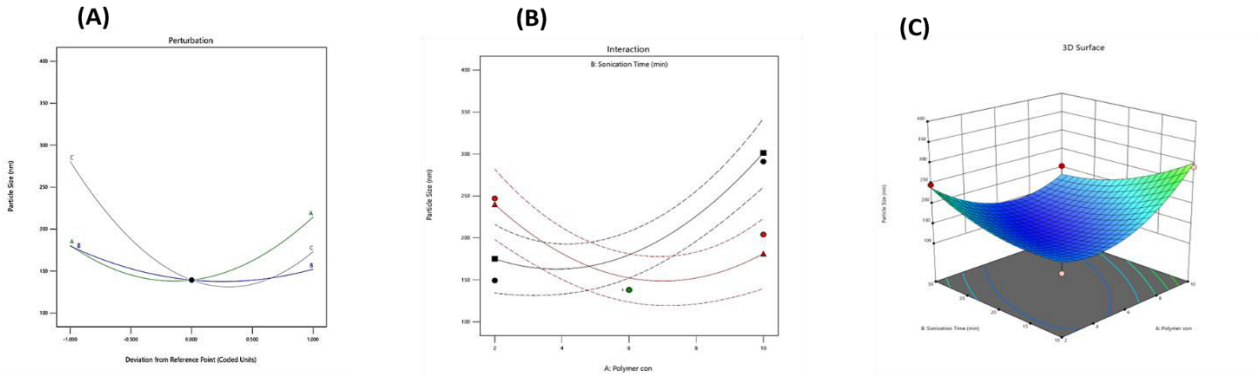

Fig. 3. Perturbation, Interaction & Predicted 3D response surface plot of Encapsulation Efficiency

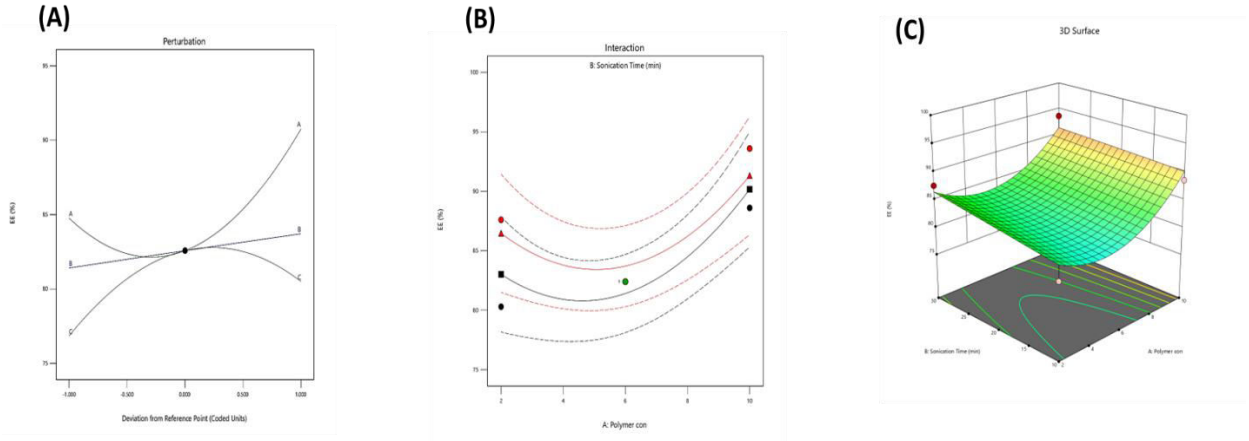

Fig. 4. Perturbation, Interaction & Predicted 3D response surface plot of Drug Release

International Journal For Advanced Research In Science & Technology
A peer reviewed international journal
www.ijarst.in
ISSN: 2457-0362

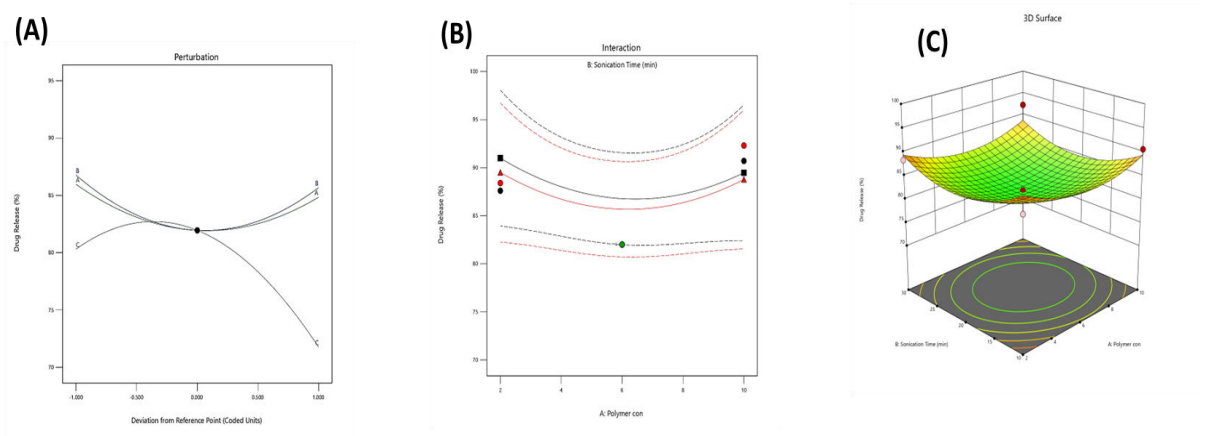

Fig. 5 (A) SEM image of the PLGA-NDP; **(B)** EDX image of the PLGA-NDP

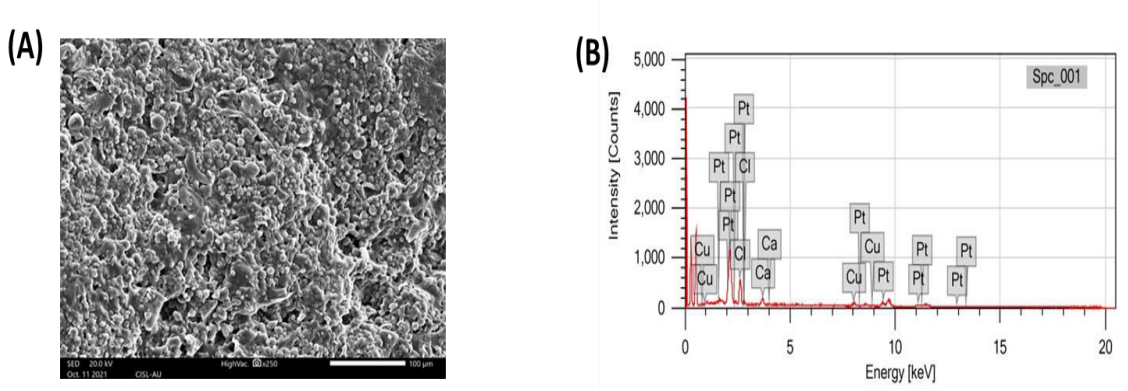

Fig. 6 Image of Thermal Analysis (TG/DTA) curve.

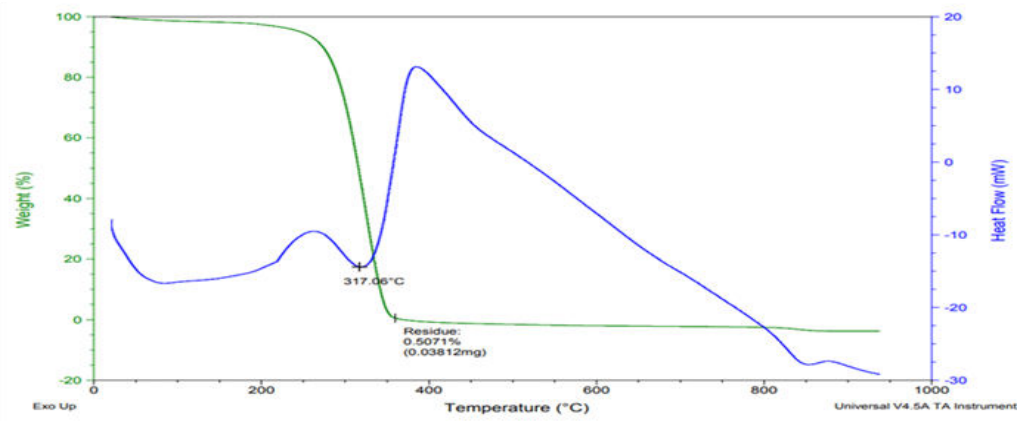

Fig. 7 Image of FTIR spectrum, (A) (B) (C) indicates the values of Nedaplatin, Cisplatin and PLGA-NDP respectively

(a)

International Journal For Advanced Research In Science & Technology
A peer reviewed international journal
www.ijarst.in
ISSN: 2457-0362

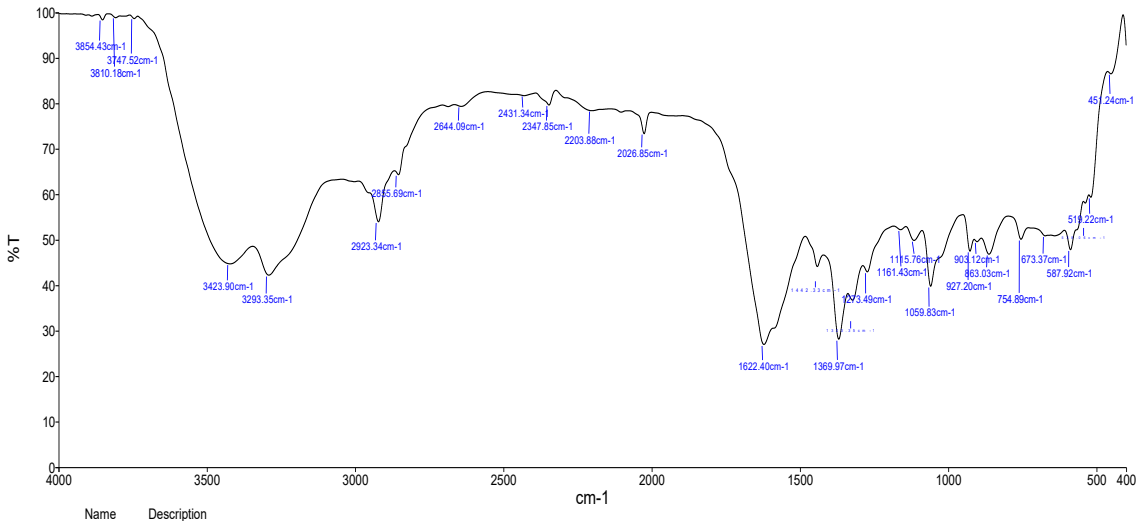

(c)

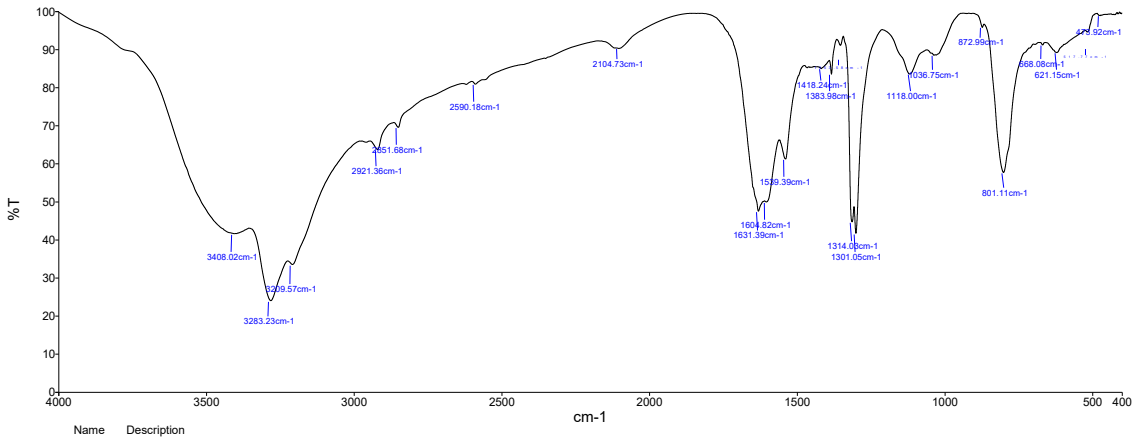

(d)

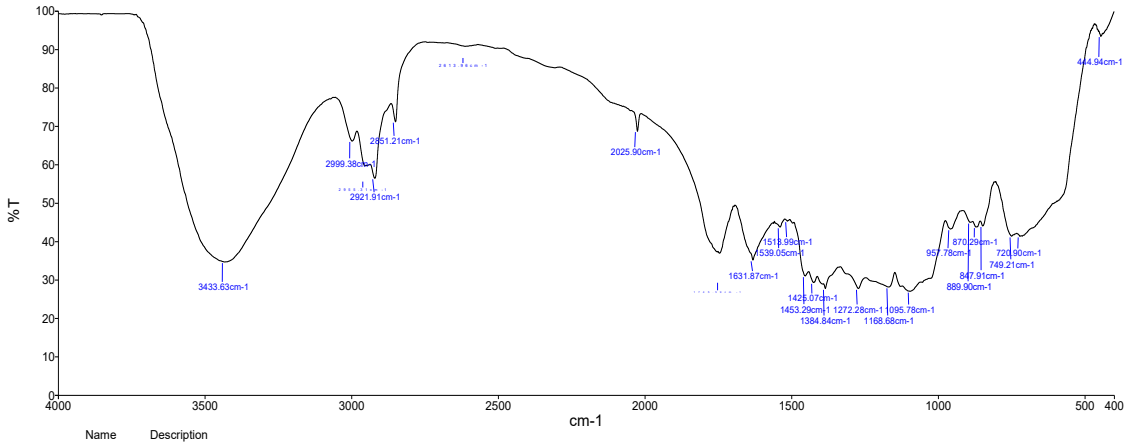

Fig. 8. Images of In Vitro Kinetic Drug Release

International Journal For Advanced Research In Science & Technology
A peer reviewed international journal
www.ijarst.in
ISSN: 2457-0362